Shaped pupil coronagraphy with WFIRST-AFTA

Alexis Carlotti[a,b], N. Jeremy Kasdin[a], Robert J. Vanderbei[c]

[a]Princeton University, MAE, Olden st., Princeton, NJ, USA;
[b]Université Joseph-Fourier, IPAG, 414 rue de la piscine, France;
[c]Princeton University, ORFE, Sherrerd Hall, Princeton, NJ, USA;

ABSTRACT

The recently completed study of using one of the AFTA telescopes for a potential WFIRST mission included a coronagraph instrument for exoplanet imaging. The challenge is to design a coronagraph that achieves the desired high contrast in the presence of the complicated on-axis optical architecture of the AFTA. This is especially difficult if contrast levels as small as 10^{-9} must be achieved at only $3\lambda/D$ from the star. In this paper we present shaped pupil designs using our new two-dimensional formulation. These designs also include constraints given by the wavefront control system, a necessary element of a complete high-contrast system in space. We have computed various shaped pupils for different contrast floors, inner working angles, and high-contrast region shapes. Two main types of masks are presented: discovery masks that offer wide discovery space with moderate inner working angles, and characterization masks which are designed for narrower discovery space and smaller inner working angles. Discovery and characterization masks would be used to image planets at different distances from the star at the same wavelengths, or to image the same planets at different wavelengths.

Keywords: Coronagraphy, High-Resolution Imaging, Exoplanet direct detection

1. INTRODUCTION

The Astrophysics Focused Telescope Assets (AFTA) are currently being considered for a potential Wide-Field InfraRed Survey Telescope (WFIRST) mission, and a recently completed study[1] includes a coronagraphic instrument to directly detect and characterize exoplanets around nearby stars. It should provide a 10^{-9} contrast at 0.2 arcsec from the star ($3\lambda/D$ for an observing wavelength λ of 800nm and a diameter D of 2.4m), and the stretch goal is 0.1 arcsec. Satisfying these requirements may be challenging because of the presence of a complicated on-axis optical architecture, and a large central obscuration of AFTA.

Many coronagraphic concepts have been studied over the past 20 years. Only recently have some of these concepts been made compatible with arbitrary telescope apertures.[2–9] Making use of at least one of these advances is mandatory in the design of a coronagraph for AFTA.

Our focus in this paper is the design of shaped pupils,[5,10,11] i.e., optimal binary apodizers that are used to create high-contrast around the star. In the particular case of WFIRST-AFTA these designs include the constraints of the AFTA pupil: central obscuration, spiders, and brackets.

An extreme adaptive optics (ExAO) system will be a necessary element of a complete high-contrast imaging instrument in space, especially if contrast as low as 10^{-9} are to be achieved. Deformable mirrors can be controlled to correct the electric field in the image plane, but they also passively increase the amplitude of the aberrations for some higher spatial frequencies. Unless this property is taken into account when designing the coronagraph, frequency mixing may result in starlight being sent in the dark zone.

The design of shaped pupils depends on many parameters. Some are set by the telescope or the wavefront control system. The others come from the high-contrast region that the mask must create: its inner and outer working angles (IWA, OWA), contrast level, and angular extent. To fully explore the parameter space we have computed apodizers for a variety of high-contrast regions.

Further author information: (Send correspondence to A.C.)
A.C.: E-mail: alexis.carlotti@obs.ujf-grenoble.fr

Techniques and Instrumentation for Detection of Exoplanets VI, edited by Stuart Shaklan, Proc. of SPIE Vol. 8864, 886410 · © 2013 SPIE · CCC code: 0277-786X/13/$18 · doi: 10.1117/12.2024096

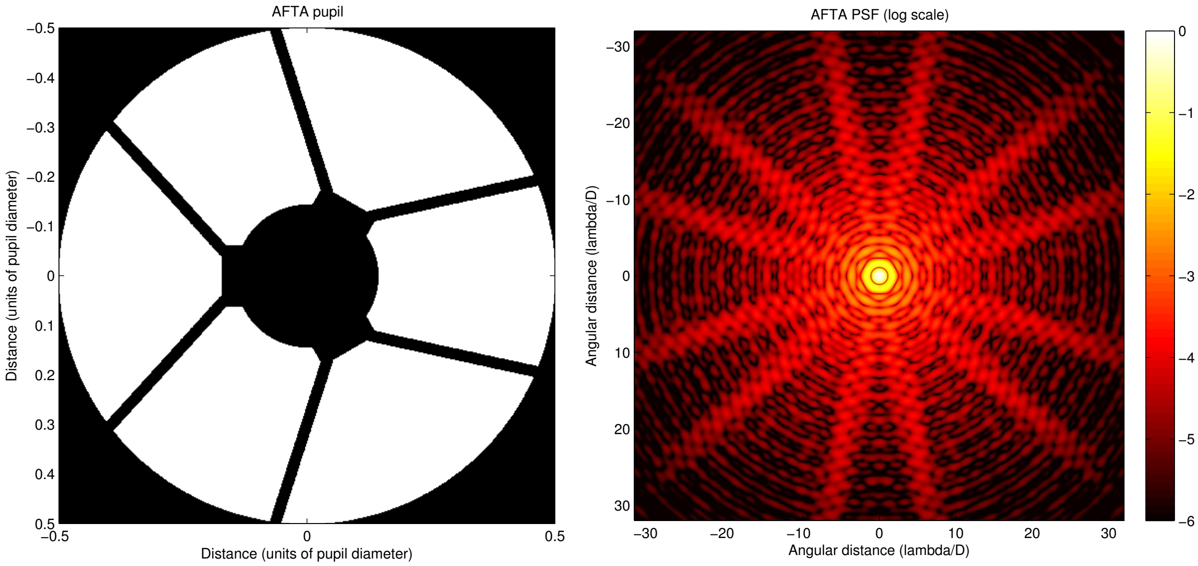

(a) (b)

Figure 1: (a): AFTA aperture used in our designs. Distances are in units of pupil diameter. (b): log scale image of the normalized PSF of the AFTA aperture. Angular distances are in units of λ/D.

Because of the nature of the AFTA aperture, shaped pupils that create 10^{-9} contrast at IWA as small as 3 λ/D in every direction have low throughputs for large OWA. To relax these constraints we have also considered shaped pupils that create high contrast in regions of the image plane with a finite angular extent. We rely on the 3-fold symmetry of AFTA to look for planets in every direction by rotating the same apodizer and observing the sky in several successive steps.

Because the IWA strongly constraints the OWA, we suggest to observe the inner and outer regions around the star with two different types of masks. Masks observing the outer region may do so with only one exposure, and we refer to them as 'discovery' masks. The inner region will have to be observed with a minimum of three exposures, using one or several 'characterization' masks.

This nomenclature comes from a usage of these masks at different wavelengths: a discovery mask with a $7\lambda/D$ IWA used at a wavelength $\lambda = 400nm$ would make it possible to observe the same region as a characterization mask with a $3.5\lambda/D$ IWA used at $\lambda = 800nm$.

In the next section we summarize the properties of the AFTA aperture and of its point-spread function. We then describe in a third section the different types of observations that a shaped pupil coronagraph would perform. In a fourth section we detail the tradeoff between IWA, OWA, contrast, and throughput for the two types of masks previously presented. The fifth section discusses the performance of combinations of discovery and characterization masks, and it draws a conclusion to the paper.

2. CHARACTERISTICS OF THE AFTA PUPIL USED IN THIS STUDY

The aperture used as a basis for our masks is showed if Fig.1a, and its point-spread function (PSF) is displayed in Fig.1b.

The central obscuration equals 29% of the diameter. The six spiders have a thickness that is 2% of the diameter. Three mounting brackets connect the six spiders to the secondary mirror. These artifacts have a significant size: they can only be covered by a 34%-large central obscuration. The aperture has a 3-fold symmetry. Note that (a) the aperture of WFIRST-AFTA may be subject to changes, and (b) the aperture we are using in this study

Twelve diffraction spikes can be seen in the image plane. Because of these the PSF of the AFTA aperture has a relatively bright diffraction halo around its center. The azymutal distance between the spikes is alternatively 24 and 35 degrees.

Apodizers that increase contrast where bright features such as diffraction spikes are located tend to have a low transmission. Higher throughputs can be sought by creating high contrast away from these bright features. Closer to the star, as the spikes merge into a halo, it becomes more difficult to create high contrast. This halo is made larger and brighter by the large number of spiders as well as by their large thickness.

We did not take into account surface errors on the primary or the secondary mirrors, and we assume here a perfect optical instrument.

3. OBSERVATION STRATEGIES

The properties of the high-contrast regions created by shaped pupils must depend on the characteristics of the AFTA pupil. For instance, the gaps between diffraction spikes along the x-axis are larger than along the y-axis (see Fig. 1b). This indicates that high-contrast should be preferentially created around the x-axis, instead of the y-axis. The optimization of shaped pupils that create identical high-contrast regions along the x- or y-axis confirms that this assumption is correct: given the same parameters, the IWA is appreciably larger when contrast is improved along the y-axis.

In addition, the way the observations will be conducted with a shaped pupil coronagraph will also be dictated by the pupil properties. The 3-fold symmetry makes it possible to rotate an apodizer by a $\pm$ 120-degrees angle. Thanks to this property, it is possible to decrease the angular extent of the high-contrast regions to 120 or 60 degrees. Observing the entire stellar environment must then be done through two or three observations using the same masks.

3.1 Divide and image

By decreasing the angular extent it is possible to decrease the IWA while keeping the same contrast and the same throughput. It may tempting to make the angular extent even smaller than 60 degrees, but three main objections can be raised against this idea: (a) the observation of the entire stellar environment would require the telescope to rotate (which is a problem both in term of instrument stability and energy consumption), or (b) the IWA would change from one observation to the other (the strength of the diffraction effects changes with the direction towards one is looking). Finally, (c) the effective throughput would be significantly smaller in the inner area of the high-contrast region (it would be smaller than the PSF FWHM).

To decrease the IWA, one can instead decrease the OWA of the high-contrast region. As illustrated in Fig.2, we propose to observe the outer region around the star with one exposure, and the inner region with 3 exposures. Two masks would be used to perform the observations: the first would be designed to create high-contrast in a region with a large IWA and a large OWA, spanning the 360 degrees around the star. The second would create high-contrast in a region with an IWA close to the $3\lambda/D$ objective, and an angular extent of 60 degrees. Its OWA could match the IWA of the previous mask.

We refer to these two different types of masks as 'discovery' masks and 'characterization' masks. The reason for this nomenclature is explained by the fact that observations at 400nm with the discovery masks and at 800nm with characterization masks would provide similar on-sky resolutions close to 0.2".

3.2 Efficiency and complementarities of the operation modes

A 60-degrees angular extent appears as the most appropriate choice for the characterization mask. Three observations are enough to cover the entire stellar neighborhood.

We have also considered shaped pupils that create 120-degrees high-contrast regions. With these masks only two observations would suffice to cover the 360-degrees around the star.

Assuming the same IWA, OWA, and contrast level are considered, choosing an M-observations solution over an N-observations solution makes sense as long as T_M/T_N, the ratio of the throughputs of the coronagraphs, is higher than M/N, or alternatively that the weighted throughput T_M/M is larger than T_N/N.

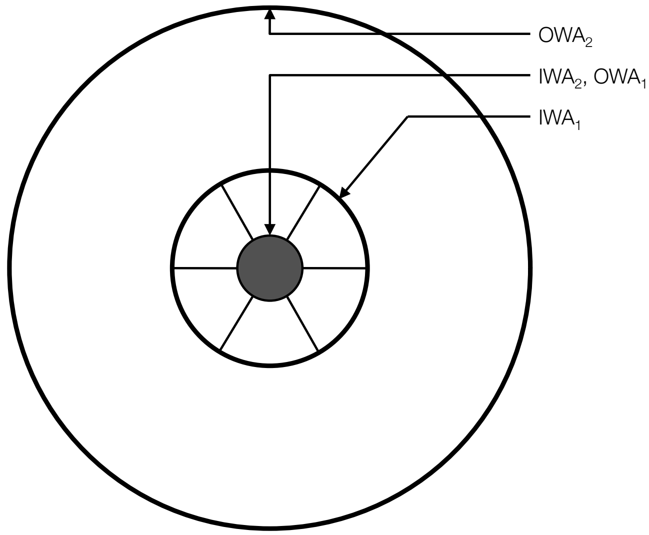

Figure 2: Cartoon of the high-contrast regions created around the star. The star itself is located at the center of the drawing, behind the dark gray disk. Two main regions are showed: an outer region and an inner region. The outer region is observed with one exposure, while the inner region is observed with three successive exposures. The outer working angle of the inner region is also the inner working angle of the outer region. It is assumed that these angles are measured in units of λ/D, or that the same wavelength and pupil diameter are used in each case.

In the case of the 120- and the 60-degrees characterization masks - for the same IWA, OWA, and contrast - the weighted throughput of the latter is 50% larger than that of the former.

Here we assume that the total time taken by an M-observations solution is directly proportional to the throughput T_M of the coronagraph. This assumption may have to be discarded to take into account the time that is required to estimate the electric field and correct the wavefront. While some extra time will add up on the observing times, the impact on the total exposure time may be lessened by the fact that less time is required to control smaller high-contrast regions.

In addition, it is not obvious that wavefront control will be successful in creating and maintaining high-contrast over the full 360-degrees region for which the discovery masks are designed. Two or potentially three observations may be required to observe the entire region.

4. EXPLORATION OF THE PARAMETER SPACE

The result of an optimization process is analyzed using two metrics that reflect the amount of energy that goes through the coronagraph:

- The apodizer transmission, i.e., the fraction of the light that gets transmitted by the apodizer.
- The effective throughput, i.e., the ratio of the energy contained in the central region of the coronagraphic PSF and the non-coronagraphic PSF. The size of this region equals the IWA of the coronagraph.

The second quantity is a more accurate measurement of the amount of light coming from the planet that will be received by the camera. Nevertheless, the apodizer transmission remains an important quantity, especially if pupil plane measurements are needed to control the wavefront.

These two metrics are not independent: high ratios between the two indicate that a significant fraction of the energy is diffracted in the image plane, which may result in higher difficulty to control the wavefront.

	OWA=$16\lambda/D$			OWA=$24\lambda/D$			OWA=$32\lambda/D$		
Contrast	Throughput			Throughput			Throughput		
	15%	20%	25%	15%	20%	25%	15%	20%	25%
10^{-7}	5.2	5.2	5.3	5.4	5.5	5.6	5.8	6.1	6.4
10^{-8}	5.7	5.7	5.8	6.3	6.4	6.8	6.7	6.9	7.5
10^{-9}	6.1	6.4	6.5	7.0	7.2	7.5	7.2	7.8	8.1

Table 1: Inner working angles in units of λ/D of the apodizers designed to create a 360 degrees high-contrast region around the star. Values are given for three different outer working angles (16, 24, and 32 λ/D), three different throughputs (15, 20, and 25%), and three different contrast (10^{-7}, 10^{-8}, and 10^{-9}).

4.1 Discovery masks

The IWA of the discovery masks is displayed in Fig.3a, 3b, and 3c for three OWA: 16, 24, and $32\lambda/D$. The IWA is plotted as a function of the contrast (x-axis) and the throughput (y-axis). The IWA increases with the throughput, and decreases with the contrast. This is expected: higher contrast values are easier to obtain than smaller ones, and if no other parameter change, smaller IWA are obtained at the expense of throughput loss.

The evolution of the IWA with the contrast and the throughput is not linear. One can look for instance at Fig.3a, where for a contrast of 10^{-8}, the IWA goes from 6 to $7\lambda/D$ when the throughput goes from 32 to 36%, and from 7 to $8\lambda/D$ when the throughput goes from 36% to 50%.

The essential information contained in these figures is summarized in Tab.1. For a 10^{-8} contrast and a 20% throughput, the smallest IWA is $5.7\lambda/D$, and it is obtained for an OWA of $16\lambda/D$.

Note that by increasing the IWA only slightly to $5.8\lambda/D$ the throughput becomes 25%. The same is not true for other OWA.

The IWA increases steadily with the OWA, and becomes $6.4\lambda/D$ for a $24\lambda/D$ OWA, and $6.9\lambda/D$ for a $32\lambda/D$ OWA. For a $24\lambda/D$ OWA, a $0.4\lambda/D$ is necessary to increase the throughput from 20 to 25%, and it becomes $0.6\lambda/D$ for a $32\lambda/D$ OWA.

For a 10^{-9} contrast, the IWA increases by an average value of $0.8\lambda/D$ for the three OWA that we have considered. For a 10^{-7} contrast, it decreases by the same amount for a 24 and $32\lambda/D$ OWA, and it decreases by $0.5\lambda/D$ for a $16\lambda/D$ OWA.

The transmission of the 10^{-8} contrast, 20% throughput masks for 16, 24 and $35\lambda/D$ are illustrated in Fig.4a,4b, and 4c. Their point-spread functions (in log scale) are showed too, in Fig.4d, 4e, and 4f. Looking at the masks, one will notice how the structures become increasingly smaller as the OWA gets larger. The masks appear to apodize the spiders and at the same time the central obscuration.

4.2 Characterization masks

The IWA of the 60-degrees characterization masks is displayed in Fig.5a, 5b, and 5c for three OWA: 16, 24, and $32\lambda/D$. As for the characterization masks, the IWA is plotted as a function of the contrast (x-axis) and the throughput (y-axis). Again, the IWA increases with the throughput, and decreases with the contrast. Something unusual can be noted in Fig.5a: for a contrast of about $10^{-7.75}$ two IWA contour lines cross each other, as if a smaller IWA mask had more throughput than a larger IWA mask. This is due to a slightly different OWA associated with the 4.25 and the $4.5\lambda/D$ IWA. While the OWA for the larger IWA is $24\lambda/D$, it is $26\lambda/D$ for the smaller IWA. This illustrates how strong an influence the OWA has on the throughput.

Tab.2 synthesizes the trade-offs information for the characterization masks. Note that is also contains information for $8\lambda/D$ OWA masks. Unsurprisingly the smallest IWA - $3.1\lambda/D$ - for a 20% throughput and a 10^{-8} contrast - is obtained for a OWA of $8\lambda/D$.

For a 10^{-9} contrast, the IWA increases by an average of $0.4\lambda/D$ for the three OWA that we have considered. For a 10^{-7} contrast, it decreases by an average of $0.5\lambda/D$.

The transmission of the 10^{-8} contrast, 20% throughput masks for 8, 16, and $27\lambda/D$ are illustrated in Fig.6a,6b, and 6c. Their point-spread functions (in log scale) are showed too, in Fig.6d, 6e, and 6f. The

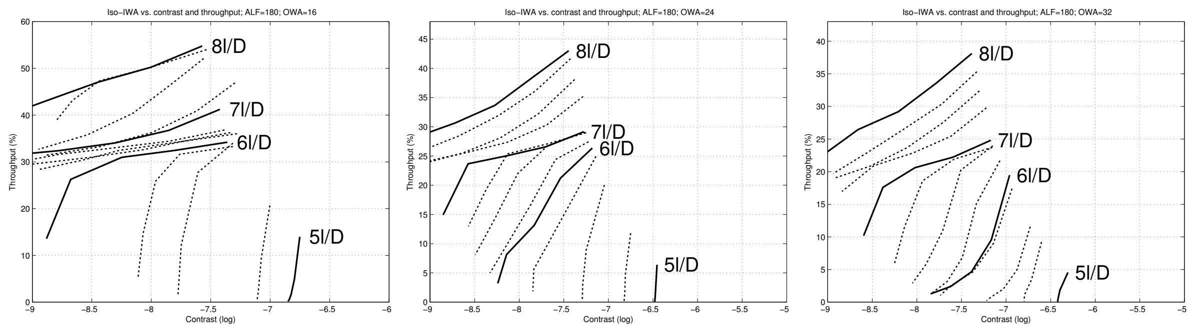

(a) (b) (c)

Figure 3: IWA contour lines for the discovery masks as a function of the contrast (log scale) and the throughput (%). Each line represents an IWA value, and the 'distance' separating two consecutive lines is $0.25\lambda/D$. The thick lines correspond to integer values of the IWA. The IWA increases with the throughput and decreases with the contrast. Its extremum values are 5 and $8\lambda/D$. (a): OWA is $16\lambda/D$. (b): OWA is $24\lambda/D$. (c): OWA is $32\lambda/D$.

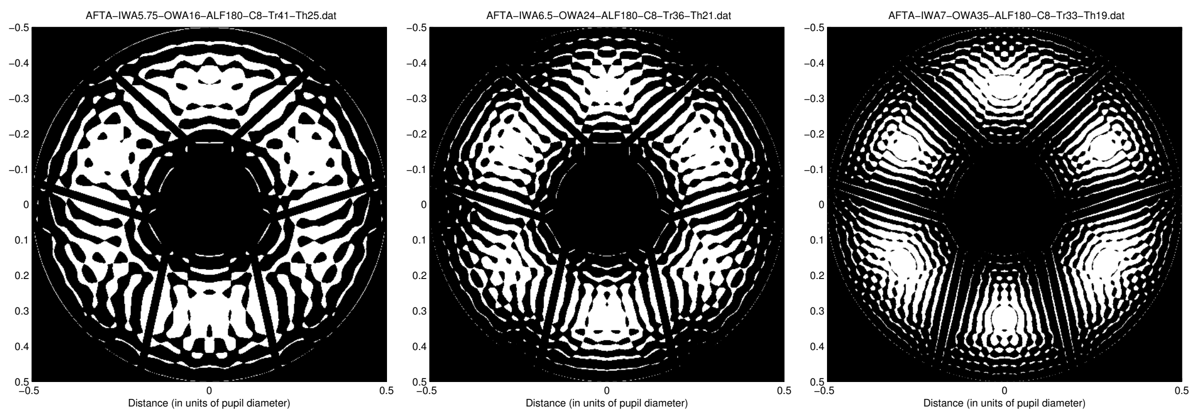

(a) (b) (c)

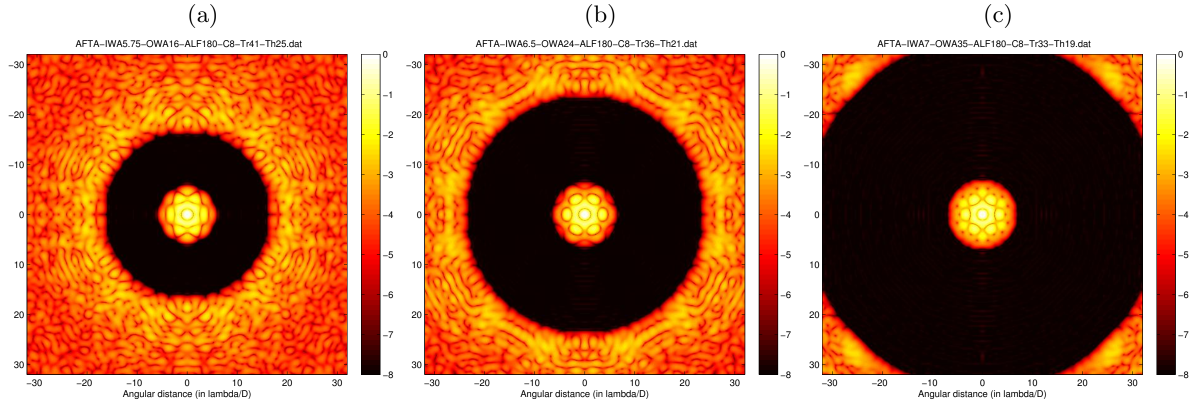

(d) (e) (f)

Figure 4: Examples of discovery masks (top) and their corresponding PSFs (bottom, log scale) for 3 OWA: 16, 24, and $35\lambda/D$. Contrast is 10^{-8}, and the respective throughputs are 25, 21, and 19%. The IWA are 5.75, 6.5, and $7\lambda/D$.

Contrast	OWA=$8\lambda/D$			OWA=$16\lambda/D$			OWA=$24\lambda/D$			OWA=$32\lambda/D$		
	Throughput			Throughput			Throughput			Throughput		
	15%	20%	25%	15%	20%	25%	15%	20%	25%	15%	20%	25%
10^{-7}	2.7	2.8	2.9	3.0	3.2	3.3	3.1	3.5	3.8	3.8	4.0	4.3
10^{-8}	3.0	3.1	3.3	3.5	3.6	3.8	3.7	4.0	4.5	4.5	4.6	4.8
10^{-9}	3.3	3.4	3.6	3.8	4.1	4.3	4.1	4.6	5.1	4.8	>5	>5

Table 2: Inner working angles (in λ/D) of the characterization masks designed to create two 60-degrees high-contrast region next to the star. Values are given for four different outer working angles (8, 16, 24, and 32 λ/D), three different throughputs (15, 20, and 25%), and three different contrast (10^{-7}, 10^{-8}, and 10^{-9}).

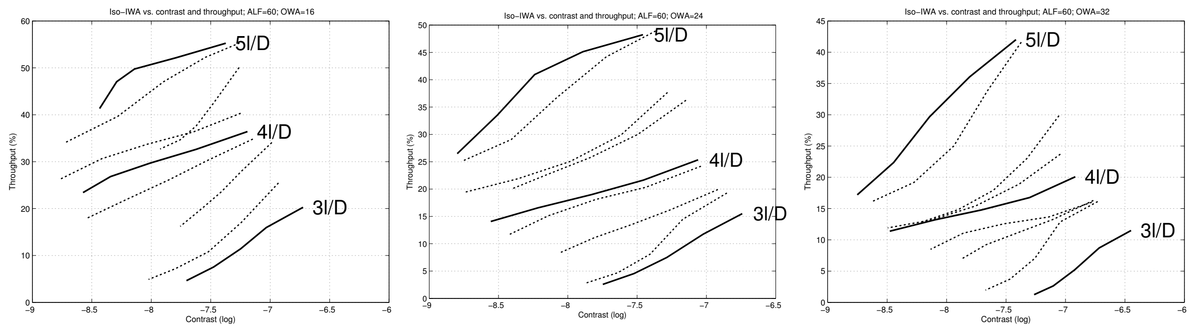

(a) (b) (c)

Figure 5: IWA contour lines for the 60 degrees characterization masks as a function of the contrast (log scale) and the throughput (%). Each line represents an IWA value, and the 'distance' separating two consecutive lines is $0.25\lambda/D$. The thick lines correspond to integer values of the IWA. The IWA increases with the throughput and decreases with the contrast. Its extremum values are 3 and $5\lambda/D$. (a): OWA is $16\lambda/D$. (b): OWA is $24\lambda/D$. (c): OWA is $32\lambda/D$.

same figures are not shown for the $32\lambda/D$ OWA: the minimum IWA is here $4.6\lambda/D$ for a 20% throughput and a 10^{-8} contrast.

5. DISCUSSION AND CONCLUSION

A coronagraphic instrument onboard WFIRST-AFTA is an exceptional opportunity for the study of planetary formation and stellar environments. The optimization techniques that we have developed make it possible to compute the apodizers that - for an arbitrary aperture - will have the highest transmission possible, while satisfying constraints that we set on the contrast in the image plane.

We have studied the performance of shaped pupil coronagraphs specifically designed for the aperture of WFIRST-AFTA, which is characterized by a 29-34% central obscuration and a 3-fold spider configuration, with a total of 6 relatively thick spiders (2% of the pupil diameter).

These elements create strong diffraction effects which are difficult to correct over broad regions of the image plane, both in term of azymutal extent, inner working angle and outer working angle.

We have mapped the parameter space to understand the tradeoffs that exist between the contrast, the throughput, the inner working angle, the outer working angle, and the angular extent of the high-contrast region.

The WFIRST-AFTA final report asks for a coronagraph with a 10^{-9} contrast at $3\lambda/D$ from the star. Getting such a small IWA with shaped pupils is challenging but it is possible. The surroundings of the star must be observed with several exposures. We suggest that an outer region be observed with one or three exposures. The complementary inner region would have to be observed with 3 exposures.

The first type of mask that we have presented is a discovery mask: it creates high contrast all around the star, and its purpose would be to observe the aforementioned outer region. For a 10^{-8} contrast, and a 20%

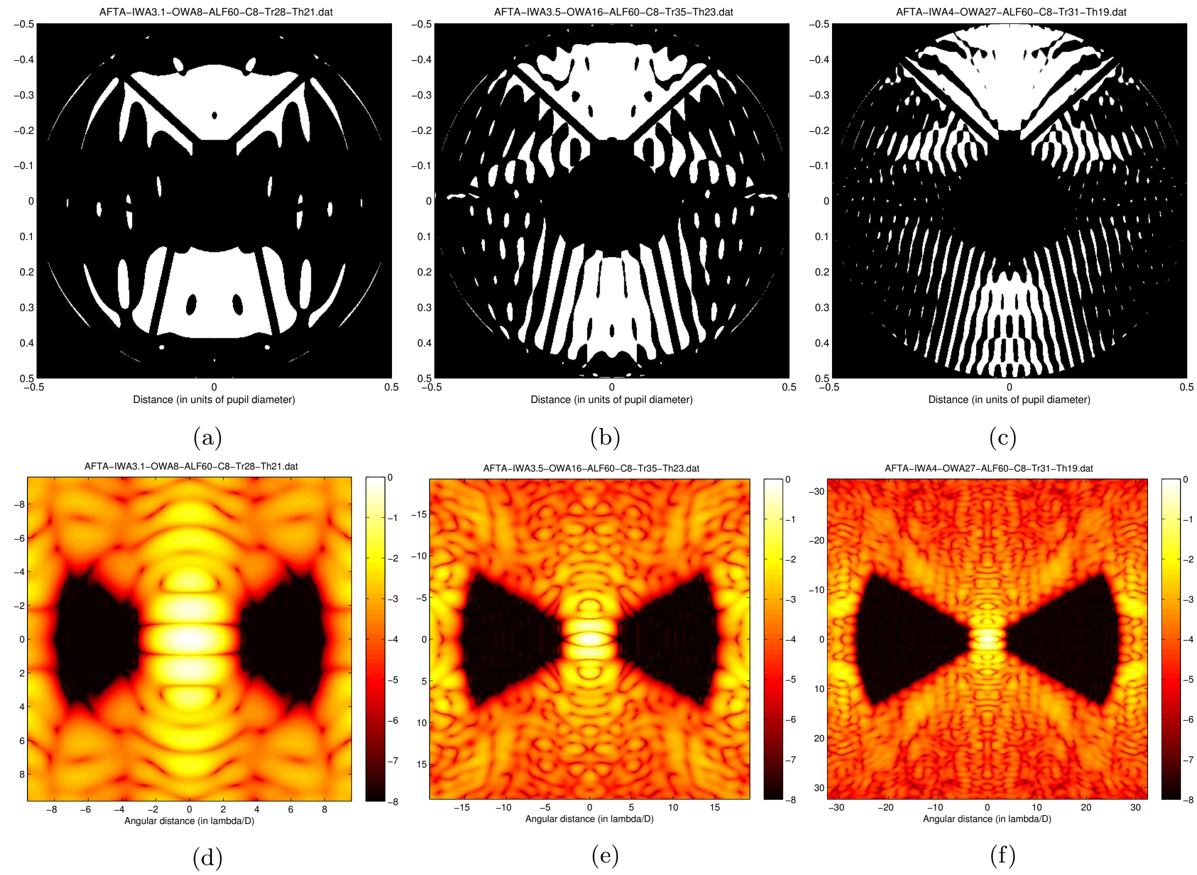

Figure 6: Examples of 20% throughput 60 degrees characterization masks (top) and their corresponding PSFs (bottom, log scale) for 10^{-8} contrast. OWA are 8, 16, and $27\lambda/D$, and IWA are 3.1, 3.5, and $4.0\lambda/D$. The exact transmission of the masks is 21, 23, and 19%.

throughput, it has a $6.5\lambda/D$ inner working angle and a $24\lambda/D$ outer working angle. For the same contrast and throughput, a larger OWA of $32\lambda/D$ results in a $7\lambda/D$ IWA.

The second type of mask we have presented is a characterization mask: it creates high contrast in a finite region closer to the star, and would thus be used to observe the inner region that surrounds it. Multiple observations are required to observe the entire stellar neighborhood. Thanks to the 3-fold symmetry of the aperture, a single shaped pupil can be used to observe the 360 degrees around the star in three observations: at each observation it creates two symmetric 60 degrees wide high-contrast regions, and the shaped pupil is rotated by $2\pi/3$ after each observation.

Masks that creates two symmetric 120-degrees wide high-contrast regions would only require two observations, but for the same IWA their throughput is too low to make them worth choosing over the 60-degrees characterization masks.

For a 10^{-8} contrast, a 20% throughput (about 33% transmission), and a $27\lambda/D$ outer working angle, our characterization mask has a $4\lambda/D$ inner working angle. Reducing the OWA to $16\lambda/D$ makes the IWA $3.6\lambda/D$, and achieving 10^{-8} contrast at $3\lambda/D$ with 20% throughput requires an $8\lambda/D$ OWA.

A complementary 60-degrees mask with an $8\lambda/D$ IWA, and a large OWA, say $32\lambda/D$ would have a 62% throughput (72% transmission). A 360-degrees mask with the same IWA, OWA, and contrast would have a 32% throughput. The IWA of the discovery mask can be decreased to $7\lambda/D$ for a 20% throughput and the same OWA.

Observing at 400nm, these IWA translates into angles of 0.1" for the characterization mask, and 0.24" for the discovery mask. At 800nm, these angles become 0.2" for the characterization mask, and 0.48" for the discovery mask. Thus, similar resolutions of 0.24" and 0.20" are obtained with the two types of masks at 400 and 800nm.

Using the full 360-degrees discovery mask over 60-degrees masks with large IWA seems to be a more efficient solution. The choice will depend on our ability to use the ExAO system to create high contrast in the entire 360-degrees region.

REFERENCES

[1] Spergel, D., Gehrels, N., Breckinridge, J., Donahue, M., Dressler, A., Gaudi, B. S., Greene, T., Guyon, O., Hirata, C., Kalirai, J., Kasdin, N. J., Moos, W., Perlmutter, S., Postman, M., Rauscher, B., Rhodes, J., Wang, Y., Weinberg, D., Centrella, J., Traub, W., Baltay, C., Colbert, J., Bennett, D., Kiessling, A., Macintosh, B., Merten, J., Mortonson, M., Penny, M., Rozo, E., Savransky, D., Stapelfeldt, K., Zu, Y., Baker, C., Cheng, E., Content, D., Dooley, J., Foote, M., Goullioud, R., Grady, K., Jackson, C., Kruk, J., Levine, M., Melton, M., Peddie, C., Ruffa, J., and Shaklan, S., "WFIRST-2.4: What Every Astronomer Should Know," *ArXiv e-prints* (May 2013).

[2] Soummer, R., "Apodized Pupil Lyot Coronagraphs for Arbitrary Telescope Apertures," ApJ **618**, L161–L164 (Jan. 2005).

[3] Soummer, R., Pueyo, L., Ferrari, A., Aime, C., Sivaramakrishnan, A., and Yaitskova, N., "Apodized Pupil Lyot Coronagraphs for Arbitrary Apertures. II. Theoretical Properties and Application to Extremely Large Telescopes," ApJ **695**, 695–706 (Apr. 2009).

[4] Soummer, R., Sivaramakrishnan, A., Pueyo, L., Macintosh, B., and Oppenheimer, B. R., "Apodized Pupil Lyot Coronagraphs for Arbitrary Apertures. III. Quasi-achromatic Solutions," ApJ **729**, 144 (Mar. 2011).

[5] Carlotti, A., Vanderbei, R., and Kasdin, N. J., "Optimal pupil apodizations of arbitrary apertures for high-contrast imaging," *Optics Express* **19**, 26796 (Dec. 2011).

[6] Martinez, P., Dorrer, C., and Kasper, M., "Band-limited Coronagraphs Using a Halftone-dot Process. II. Advances and Laboratory Results for Arbitrary Telescope Apertures," ApJ **744**, 79 (Jan. 2012).

[7] Carlotti, A., "Apodized phase mask coronagraphs for arbitrary apertures," A&A **551**, A10 (Mar. 2013).

[8] Guyon, O., Hinz, P. H., Cady, E., Belikov, R., and Martinache, F., "High Performance Lyot and PIAA Coronagraphy for Arbitrarily shaped Telescope Apertures," *ArXiv e-prints* (May 2013).

[9] Pueyo, L. and Norman, C., "High-contrast Imaging with an Arbitrary Aperture: Active Compensation of Aperture Discontinuities," ApJ **769**, 102 (June 2013).

[10] Spergel, D. and Kasdin, J., "A Shaped Pupil Coronagraph: A Simpler Path towards TPF," in [*American Astronomical Society Meeting Abstracts*], *Bulletin of the American Astronomical Society* **33**, 1431 (Dec. 2001).

[11] Vanderbei, R. J., Spergel, D. N., and Kasdin, N. J., "Circularly Symmetric Apodization via Star-shaped Masks," ApJ **599**, 686–694 (Dec. 2003).